International Journal of Engineering Research-Online
A Peer Reviewed International Journal
Articles available online http://www.ijoer.in

Vol.3., S3, 2015

NCERFM-2015

ISSN: 2321-7758

STRUCTURAL AND OPTICAL PROPERTIES OF EUROPIUM DOPED ALKALINE EARTH ZINC BISMUTH BORATE GLASSES

[1]RAMESH BODA*, [2]SRINIVAS.G, [3]KOMARAIAH.D, [4]SHAREEFUDDIN. MD, [5]M.N CHARY, [6]SAYANNA.R

[1]scholar, [2]scholar, 3scholar, [4]Asst.professor, [5]Professor, [6]Professor

Department of physics, Osmania University, Hyderabad-07, Telangana, India.

Corresponding author Mailing address:

Ramesh Boda

Email: ramesh.777eu@gmail.com

ABSTRACT

Europium doped alkaline earth zinc bismuth borate glasses with the composition xSrO-15ZnO- $20Bi_2O_3$- (63−x) B_2O_3- 2EuO [where x= 0, 5, 10, 15, 20 mol %] were prepared by the melt quenching technique. The amorphous nature of the prepared glasses was confirmed by X-ray diffraction studies. The glass transition temperature (T_g) values were evaluated from the differential scanning calorimetry (DSC) thermograms. By using the Archimedes principle, the density of the samples was evaluated. Molar volume was calculated from the density data. The structural changes in the boron and bismuth co-ordination with composition were investigated by FT-IR spectroscopic techniques. The optical absorption spectra were recorded in the wave length range 200-900nm. Cutoff wavelengths, direct, indirect band gaps, Urbach energies, Molar refraction (R_m), Molar electronic polarizability (α_m), reflection loss and refractive index values were evaluated.

Key words: Bismuth borate glass, XRD, UV, FTIR, Density, Molar volume.

1. INTRODUCTION:

Glasses containing Bi_2O_3 have attracted considerable attention because of their wide applications in the field of glass-ceramics, thermal and mechanical sensors, reflecting windows, radiation shielding. They can be used as layers for optical and opto-electronic devices. Bismuthate glasses containing alkali oxide act as ionic conductors and possess high conductivity compared to other heavy metal glasses. Among different glass matrices, scientific interest on bismuth borate glasses is attributed to their favorable properties such as rigid physical and chemical stability, high refractive index, extensive glass formation range, long infrared cutoff and large third order nonlinear optical susceptibility, low melting temperature, high density and high infrared transparency. Bismuth borate glasses are also possessing broad range of applications in the fields of optical fiber amplifiers, thermal and mechanical sensors, laser materials, electro-optic switches, optoelectronics and magneto optical devices, reflecting windows, glass ceramics, photonic switches and layers for optical and electronic devices etc. In The present form of alkaline earth zinc bismuth borate (ZSB) glasses doped with Europium oxide, the oxides such as Bi_2O_3 and ZnO could be found as the network modifiers (NWM) with relatively large composition range and B_2O_3 can be used as the network former (NWF) and is contained in most of the important commercial glasses.

2. Materials and methods:

2.1. Glass preparation:

Reagent grade H_3BO_3, Bi_2O_3, ZnO and SrO with EuO as dopent were used as the starting materials for preparing the glasses having the compositions xSrO-15ZnO- $20Bi_2O_3$- (63−x)B_2O_3- 2EuO [where x= 0, 5, 10, 15, 20 mol %] For each composition, the raw materials in the powder form were mixed using a mortar and pestle. Each mixture was put in muffle furnace melted in a porcelain crucible at 1000°C for 3–4 hour in air. The glass melts were stirred occasionally to achieve good homogeneity. The highly viscous melt was cast in to a cylindrically shaped mold of stainless steel. The glass produced was annealed at 200°C in a second furnace for 2 hr after which the furnace was switched off and the glass was allowed to cool gradually for 2 hrs.

2.2. XRD

Shimadzu X Ray Difractometer model powder x-ray Difractometer with copper k tube target operated at 40 kV, 30mA was used to record the x-ray diffractograms. All the x-ray diffractograms were recorded at room temperature. All the recorded peak free x-ray diffractograms confirmed [fig.1] the amorphous nature of the samples, prepared in the present studies.

2.3. Density:

The densities of these glass samples were determined at room temperature by the Archimedes principle using xylene as an immersion liquid. The density () was then calculated from the following formula:

$$\rho = \frac{w}{w - w_1}\rho_x$$

where w is the weight of the glass sample in air, w1 is the weight of the glass sample when immersed in xylene of density (ρ_ξ) 0.865gm/cm^3 at room temperature (30^{o}C). The reported values of density represent the average of 3 determinations using different samples for each composition.

2.4. The DSC:

The differential scanning calorimetry (DSC) thermograms were recorded using DSC Q20 V24.10 Build 122 Instrument, with heat flow (mW) at the rate of 10.00 °C/min, Equilibrate at 50 °C to 520 °C temperature in Ramp. 3mg of Sample in powder form is taken in to Tzero Aluminum Pan and lid under liquid Nitrogen Gas pressure of 50.0 ml/min.

2.5. Optical absorption:

The optical absorption spectra of the polished samples (thickness 2.00mm) were recorded at room temperature using recording spectrophotometer make by Analytical Technologies Limited (Philip halogen, deuterium lamp(200H),model: Spectro UV 2092) in the range 200–900nm.

3. Results and discussion:

3.1. The density and molar volume

The density verses mol% of SrO graph gave a non linear relation and the molar volume was calculated from the density data, using the formula

$$V = \frac{M}{\rho}$$ where M = average molecular weight, ρ = Density.

The molar volume verses mol% of SrO graph (fig.2) gave a non linear relation.

3.2. The DSC

The glass transition temperature of samples is evaluated from DSC graphs (fig.3) and the values of transition temperatures [table.3] are found to be around 447 to 472 centigrade's from which the glassy nature of samples is confirmed, as the mole percentage of Strontium is increasing the transition temperature is decreasing.

3.3. Infrared spectra

FTIR transmittance spectra [fig.4]showed fine intense absorption bands centered around 1800, 1340, 920, 692 and 520 cm^{-1} and small shoulders around 270,350, 420, 1740, 2300, 2920 and 3400 cm^{-1}.

The sharp intense band around 1340 cm-1 and showed around 1390 cm^{-1} are due to symmetric stretching vibration of B-O bonds in BO_3 units varied from Pyro, Ortho borate groups respectively.

A sharp band around 1359 cm^{-1} are due to B-O symmetric stretching vibration in BO_3 units from Pyro and Ortho borate groups.

The sharp band around 692 cm-1 is due to the bending vibrations of B-O-B units in BO_3 triangles.

The broad intense band around 920 cm-1 is assigned to stretching vibrations of BO_4 units in various structural groups.

2920 cm-1 and 3020 cm-1 presence of hydroxyl or water groups present in the glass.

The absence of peak at 806 cm-1 indicates the absence of Boroxol ring in vitreous B_2O_3 glasses, 883 cm-1 band is due to Bi-O and /or Bi-O-Bi in [BiO_6] octahedral.

The peak at 705 to 713 cm^{-1} is due to B-O-B bending in oxygen bridges between two trigonal boron atoms.

Table.1:Observed IR absorption band in Eu^{3+} ions doped alkaline earth oxide Zinc bismuth borate glasses

S.No	Sample name	IR absorption bands										
1	SrZnBiBEu 0	264	352	470	516	692	904	1340	1363	1734	1799	2306
2	SrZnBiBEu 5	279	352	420	516	696	920	1338	1359	1747	1842	2308
3	SrZnBiBEu 10	279	352	420	516	705	883	1338	1359	1747	1799	2309
4	SrZnBiBEu 15	279	372	420	522	709	881	1340	1359	1772	1863	2305
5	SrZnBiBEu 20	281	354	420	522	713	883	1317	1334	1666	1863	2306

Table.2. Vibration types of different IR wave numbers.

Range of wave numbers (cm^{-1})	Vibration types
420–522	Bi–O–Bi stretching vibration of [BiO_6] octahedral [2, 1]
692–713	Bending vibration of BO_4 units [2, 1]
881–920	Stretching vibration of [BO_4] units [1, 2]
1317–1363	Stretching vibration of B–O–B in [BO_3] triangles [1, 2]
1600-1800	Bending modes of OH groups [2]
2304-2380	Anti symmetric stretching of water molecule [2]
2620-2920	Hydrogen bonding [1]
3400-3460	O-H stretching vibration [1]

Table.3.Absorption cutoff wavelengths, Indirect BG, Direct BG, Urbach Energy from UV data.

S.N	Sample name	cutoff wave length	r=1/2	r=1/3	r=2	r=2/3	Urbach Energy	Reflection loss	Refractive index	R_m (cm^3)	α_m (10^{-24}) ($Å^3$)	Density (gm/cm^3)	M. Vol (cm^3)	A.M.W (gm)	Tg (°C)
1	ZSB 0	423	2.715	2.726	2.923	2.870	0.367	0.621	2.428	17.693	7.0	5.3137	28.491	151.392	472
2	ZSB 5	444	2.655	2.743	2.884	2.818	0.244	0.6205	2.432	18.135	7.19	5.2787	29.2271	154.281	471
3	ZSB 10	430	2.616	2.778	2.951	2.888	0.238	0.616	2.411	17.653	6.999	5.4843	28.6577	157.167	464
4	ZSB 15	428	2.578	2.692	2.872	2.790	0.305	0.6212	2.433	18.0	7.137	5.5201	28.9964	160.063	449
5	ZSB 20	442	2.585	2.687	2.867	2.798	0.315	0.6214	2.434	18.0	7.137	5.625	28.9688	162.950	447

3.4. Optical absorption

The Optical absorption spectra of the glass composition xSrO-15ZnO- $20Bi_2O_3$- (63−x) B_2O_3- 2EuO is shown in frg.8. From the optical absorption spectra we observe only one broad absorption band. It is clear from the fig.7 that the absorption edges were not sharp which is an indication of amorphous nature of the glass samples. The absorption coefficient, α (υ) is determined near the absorption edge of different photon energies for all glasses and is given by the relation;

$$\alpha(\upsilon) = \frac{A}{d}$$

Where 'A' is the absorbance and'd' is the thickness of the sample. Davis and Mott proposed the following relation for amorphous materials where the absorption co-efficient α (υ) is a function of photon energy (hυ) for direct and indirect transitions.

$$(\alpha h\upsilon) = B^2(h\upsilon - E_g)^r$$

Where E_g, is the optical band gap, and 'r' is the index which has different values (2, 2/3, l/2 and 1/3) corresponding to indirect allowed, indirect forbidden, direct allowed and direct forbidden transitions, respectively. B is a constant called the band tailing parameter and υ is the energy of incident photons. Here the optical band gap refers to photons assisting the electrons to move from valence band to conduction band. The optical band gap between valence band and conduction band in oxide glasses can be determined from the position of the absorption edge. The absorption edge gives information about the width of the localized states in the band gap which arises due to disorder in the glass matrix. The optical band gap energy also provides information about the nature of chemical bonds and glass structure. The typical $(\alpha h\upsilon)^{1/2}$ versus photon energy (hυ) [fig.5]for direct allowed transitions, $(\alpha h\upsilon)^{2/3}$ versus (hυ) for indirect forbidden[fig.10], $(\alpha h\upsilon)^{1/3}$ versus (hυ)

for direct forbidden[fig.9] and $(\alpha h\upsilon)^2$ versus $(h\upsilon)$ [fig.6] indirect allowed transitions (called as Tauc's plot) have been plotted to find the values of optical band gap energy, E_g. The values of E_g are obtained by extrapolating the linear region of the curve to the (x) axis, i.e. $(\alpha h\upsilon)^{1/2}=0$ and $(\alpha h\upsilon)^2=0$ for indirect and direct transitions and is shown in Figs.5,6. The values of E_g for absorption edge, indirect allowed transitions and direct allowed transitions are given in Table 3.

The value of band gap can be obtained by extrapolating the linear region of $(a/\lambda)^{1/r}$ verses (l/λ) curve at $(a/\lambda)^{1/r}=0$. The x-axis intersect value is multiplied with 1239.83 then it is found that the best fit is observed for r=2. This value of band gap, designated as E_{opt}^{asf} in eV, is calculated from the parameter λ_g using the expression

$$E_{opt}^{asf} = \frac{1239.83}{\lambda g}$$

The variation of $(a/\lambda)^{1/r}$ verses $(1/\lambda)$ is shown in Fig.5. The values of optical band gaps E_{opt}^{asf} of the present glass samples calculated using ASF method are reported in Table 3. It is observed that the values of optical band gap energy (E_g) match the values of optical band gap energies E_{opt}^{asf} calculated from ASF method.

3.5. Urbach Energy

The Urbach energy, ΔE is defined as the energy gap between localized tail states in the forbidden band gap. It provides a measure of disorder in the amorphous and crystalline solids. In amorphous materials, structural disorder dominates and this could be due to the presence of structural defects like dangling bonds or non bridging oxygen atoms. In borate based glass network, the higher the concentration of NBO's, the smaller is the optical band gap energy and the greater are the Urbach energy values. The ΔE values are evaluated from the Urbach plots [Fig.8] of ln (α) versus (hυ) by taking the reciprocal of the slopes of the linear portion of the curves and are listed in Table.3. The variation Urbach energy (ΔE) with SrO concentration is non- linear with increase of SrO content.

3.6. Refractive Index

Refractive index (n) is determined from optical band gap energy (E_g) using the formula proposed by Dimitrov and Sakka

$$\frac{(n^2-1)}{(n^2+2)} = 1 - \sqrt{\frac{E_{opt}^{asf}}{20}}$$

The refractive index (n) values calculated from above Equation and are given in Table 3. The refractive index values of the present glass samples are in the range 2.411 to 2.434. The refractive index values quoted correspond to the respective alues of the present glass samples. However there are chances of creeping small errors in the refractive index "n" values owing to extrapolation $(a\lambda^{-1})^{1/2}$ verses (λ^{-1}) plots in estimating E_{opt}^{asf} .

3.7. Molar refraction (R_m)

The product of both reflection loss and molar volume is called molar refraction R_m (cm^3). This parameter is related to the structure of the glass is given by the Lorentz- Lorentz equation where R_m is directly proportional to V_m as follows

$$R_m = \left(\frac{n^2-1}{n^2+2}\right) V_m$$

Where "n'' is the refractive index, V_m is molar volume and the term $(n^2-1)/(n^2+2)$ represents the reflection loss. The values of molar refraction R_m are presented in Table.3.

3.8. Molar electronic polarizability (α_m)

According to Clausios-Mosotti, the molar electronic polarizability α_m is given by the relation

$$\alpha_m = \left(\frac{3}{4\pi Na}\right) R_m$$

where Na is Avogadro's number.

The values of molar electronic polarizability α_m are presented in Table 3.

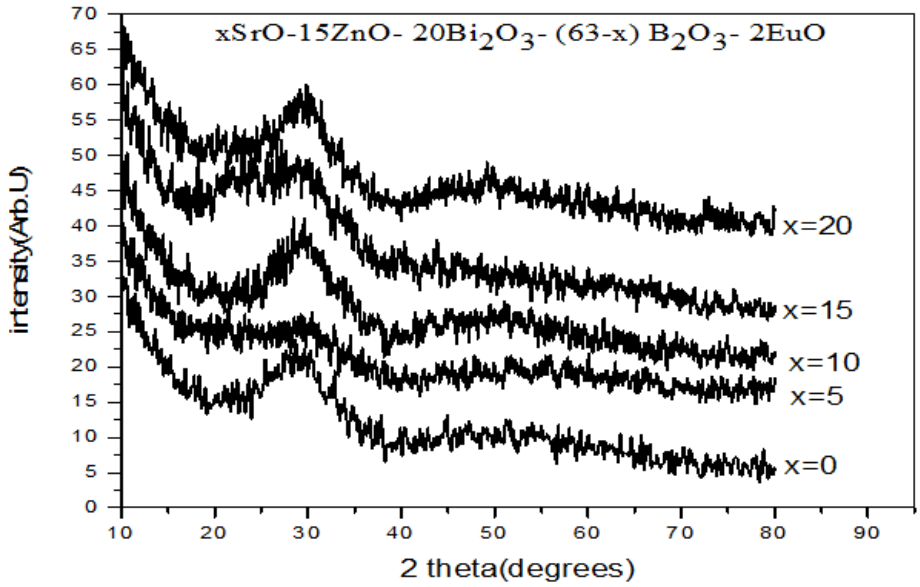

Fig.1.XRD of doped glasses

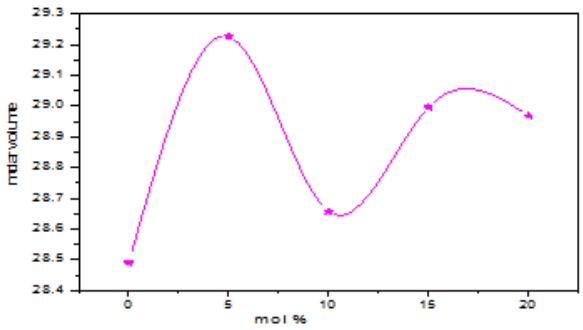

Fig.2.molar volume Vs mol % of SrO

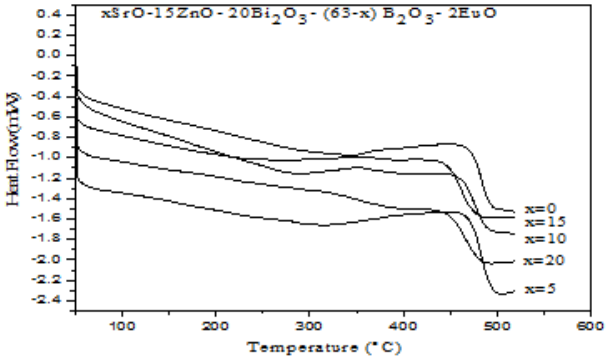

Fig.3.DSC: Temperature Vs heat flow

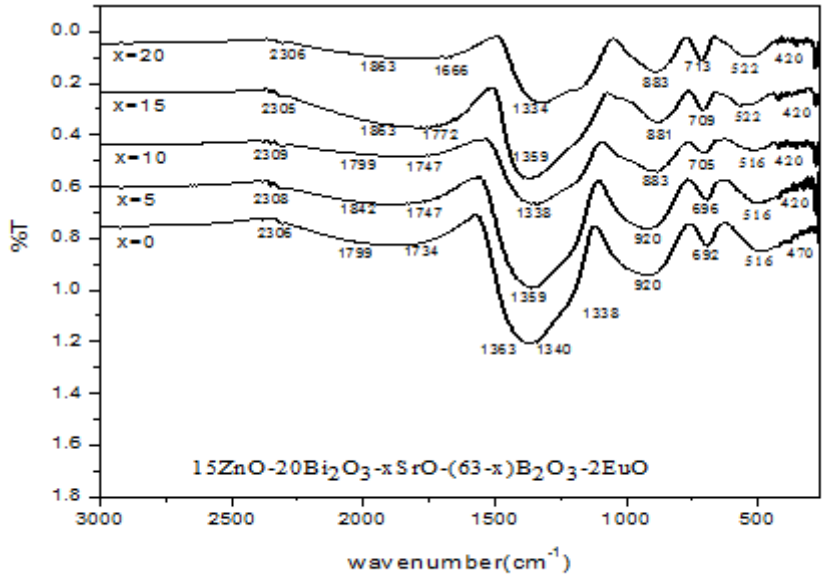

Fig.4. FTIR transmittance spectra

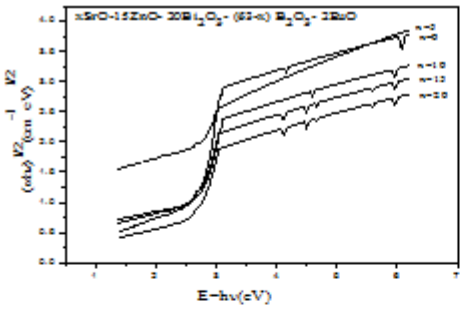

Fig.5.Tauc's plots $(\alpha h\upsilon)^{1/2}$ verses $(h\upsilon)$

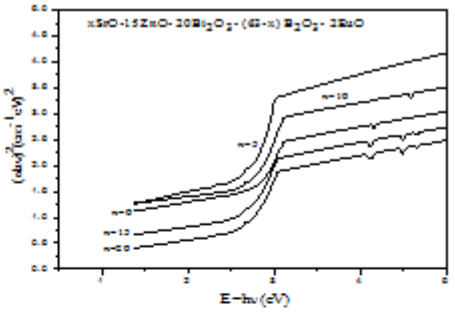

Fig.6: Tauc's plots $(\alpha h\upsilon)^{2}$ verses $(h\upsilon)$

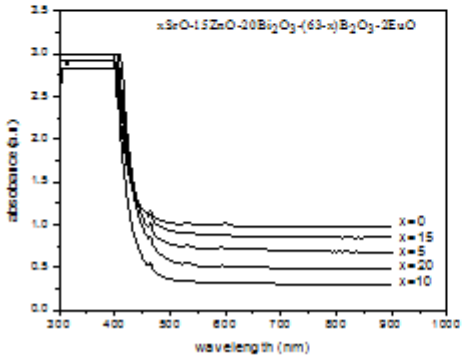

Fig.7: Cutoff wavelengths from UV graph

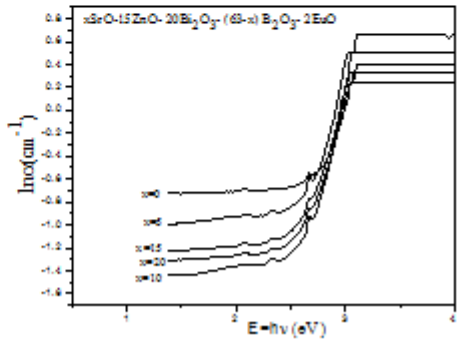

Fig.8: Urbach's plots ln (α) verses $(h\upsilon)$

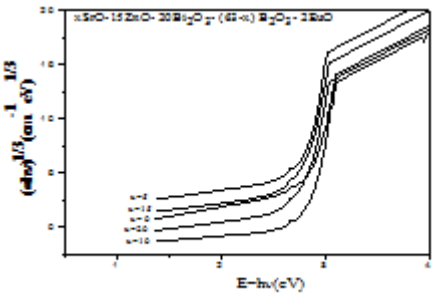

Fig.9.Tauc's plots $(\alpha h\upsilon)^{1/3}$ verses $(h\upsilon)$

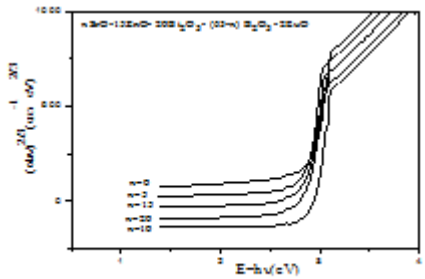

Fig.10.Tauc's plots $(\alpha h\upsilon)^{3}$ verses $(h\upsilon)$

4. Conclusions:

The bismuth borate oxide glasses of composition xSrO-15ZnO- $20Bi_2O_3$- (63−x) B_2O_3- 2EuO revealed that the XRD results shows that the investigated samples are amorphous in nature.

The presence of peaks varying with positions. The glass transition temperature (T_g) from (DSC) thermograms which confirm the glass. The FTIR studies revealed that in the glass matrix various borate groups are randomly interconnected typical borate groups like ortho borate glasses were observed. From FTIR spectra it is also evident that present glasses consist of pyro, ortho BO_3 and octahedral BiO_6 structural units. From the optical data the evaluated values of optical band gap energy (E_g) matches with the values of optical band gap energies E_{opt}^{asf} calculated from ASF method. The variation of Urbach energy (ΔE) with SrO concentration is varying non-linearly with increase of SrO contents.

5. Acknowledgements:

Authors are thankful to UGC New Delhi for providing financial support, by awarding fellowship under RGNF.

6. References:

[1] Pal.I, Agarwal.A, Sanghi.S, Aggarwal.M.P, Optical Materials 34 (2012) 1171–1180.

[2] Joao Coelho, Cristina Freire, Sooraj.N, Hussain. Spectrochimica Acta Part A 86 (2012) 392– 398.

[3] Rani.S, Sanghi.S, Agarwal.A, Seth.V.P, Spectrochimica Acta Part A 74 (2009) 673–677.

[4] Karakassides.M.A, Saranti.A, Koutselas.I, J. Non-Cryst. Solids 347 (2004) 69.

[5] Sene.F.F, Martinelli.J.R, Gomes.L, J. Non-Cryst. Solids 348 (2004) 63.
[6] Campbell.J.H, Suratwala.T.I, J. Non-Cryst. Solids 263 (2000) 318.
[7] Donald.I.W, Metcalfe.B.L, Fong.S.K, Gerrard.L.A, J. Non-Cryst. Solids 352 (2006) 2993.
[8] Bingham.P.A, Hand.R.J, Forder.S.D, Mater. Res. Bull. 41 (2006) 1622.
[9] Fang.Y, Hu.L, Liao.M, Wen.L, J. Alloys Compd. 457 (2008) 19.
[10] Lee.E.T.Y, Taylor.E.R.M, Opt. Mater. 28 (2006) 200.
[11] Abo-Naf.S.M, El-Amiry.M.S, Abdel-Khalek.A.A, Opt. Mater. 30 (2008) 900.
[12] Chen.W.S, Monroe.E.A, Condrate Sr. R.A, Guo.Y.M, J. Mater. Sci.: Mater. Med.4 (1993) 111.
[13] Kokubo.T, Yoshihara.S, Nishimura.N, Yamamuro.T, Nakamura.T, J. Am. Ceram.Soc. 74 (1991) 1793.
[14] Arul Rayappan.I, Selvaraju.K, Marimuthu.K, Optical Materials 34 (2012) 1171–1180.
[15] Rajyasree.Ch, Bala Murali Krishna.S, Ramesh Babu.A, Krishna Rao.D, Journal of Molecular Structure 1033 (2013) 200–207.
[16] Gaurav Gupta, Atul D.Sontakke, Karmakar.P, Biswas.K, Balaji.S, Saha.R, Sen.R, Annapurna.K. Journal of Luminescence 149 (2014)163–169.
[17] Gaafar.M.S, Marzouk.S.Y, Zayed.H.A, Soliman.L.I, Serag El-Deen.A.H, Current Applied Physics 13 (2013) 152e158.
[18] Petru Pascuta, Simona Rada, Gheorghe Borodi, Maria Bosca, Lidia Pop, Eugen Culea. Journal of Molecular Structure 924–926 (2009) 214–220.
[19] Srinivasa Rao.N, Srinivasa Rao.L, Gandhi.Y, Ravikumar.V, Veeraiah.N, Physica B 405 (2010) 4092–4100.
[20] Karthikeyan.B, Mohan.S, Physica B 334 (2003) 298–302.
[21] Limkitjaroenporn.P, Kaewkhao.J, Limsuwan.P, Chewpraditkul.W, Journal of Physics and Chemistry of Solids 72 (2011) 245–251.
[22] Swapna.K, Mahamuda.Sk, Srinivasa Rao.A, Shakya.S, Sasikala.T, Haranath.D, Vijaya Prakash.G, Spectrochimica Acta Part A: Molecular and Biomolecular Spectroscopy 125 (2014) 53–60
[23] Marzouk.M.A, Journal of Molecular Structure 1019 (2012) 80–90.
[24] Rajyasree.Ch, MichaelVinayaTeja.P, Murthy.K.V.R, KrishnaRao.D, Physica B 406 (2011) 4366–4372.